Int. J. Heat Mass Transfer. Vol. 27, No. 10, pp. 1865–1872, 1984
Printed in Great Britain

0017-9310/84 $3.00 + 0.00
Pergamon Press Ltd.

Spectral transmission and reflection properties of high temperature insulation materials

R. CAPS, A. TRUNZER, D. BÜTTNER and J. FRICKE
Physikalisches Institut der Universität Würzburg, D-8700 Würzburg, Federal Republic of Germany

and

H. REISS
Brown, Boveri & Cie. AG., Zentrales Forschungslabor, D-6900 Heidelberg, Federal Republic of Germany

(*Received* 7 *November* 1983 *and in revised form* 23 *January* 1984)

Abstract—This paper describes two approaches for the determination of radiative flux in high temperature insulations: (a) optical transmission and reflection studies; (b) application of rigorous Mie scattering theory and Monte Carlo simulations of both calorimetric and optical measurements. It is shown that the wavelength resolved extinction coefficient *and* the first-order term of the scattering phase function series expansion are indispensible parameters for an optimization of the insulation properties of anisotropically scattering insulation. The paper demonstrates the validity of the diffusion approximation for radiative transfer also for strong anisotropic scattering. A study of the extinction properties of different opacifiers is added.

1. INTRODUCTION

THE DEVELOPMENT of a high temperature insulation of low thermal conductivity requires a large optical thickness, τ_0, throughout the IR spectrum (e.g. $\tau_0 = 500$ for a temperature of 600 K at the hot side of the insulation for a radiative heat flux below 20 W m^{-2}). For an evacuated insulation this usually allows the total heat flux, $\dot{q}$, to be calculated as the algebraic sum of a solid conduction part, $\dot{q}_{sc}$, and radiation heat flux, $\dot{q}_{rad}$

$$\dot{q} = \dot{q}_{sc} + \dot{q}_{rad}.$$

From the diffusion solution of radiation transfer this yields

$$\dot{q} = -(\lambda_{sc} + \lambda_{rad}) \cdot \mathrm{d}T/\mathrm{d}x$$
$$= -(\lambda_{sc} + 16n^2\sigma T^3/3E) \cdot \mathrm{d}T/\mathrm{d}x \quad (1)$$

where n is the effective index of refraction (real part), σ the Stefan–Boltzmann constant and E the total extinction coefficient, i.e. the sum of the absorption and scattering coefficient. The aim of this paper is to report on our investigations on how to determine and minimize $\dot{q}_{rad}$. These investigations include:

(a) measurements of transmission and reflection spectra for fibre insulations and for different opacifiers in the wavelength range $2.5 \leqslant \Lambda \leqslant 14.5$ μm,

(b) determination of extinction coefficients, albedo, and the amount of forward scattering from experimental data by means of improved solutions of the equation of transfer which are superior in accuracy to frequently used two-flux models,

(c) calculation of specific extinction properties, scattering phase functions and albedo from rigorous Mie theory as well as comparison of measured and calculated IR spectra,

(d) check on the results achieved so far on radiative transfer by means of a Monte Carlo simulation for multiple and anisotropic scattering.

Improving IR extinction or reflection by optimized particle diameters has its well-known optical parallel in improving the diffuse reflectance of white paints by a selection of pigment particles with an optimum diameter [1]. Choosing thermal insulation components with respect to the same criterion has qualitatively been discussed in low temperature insulation development [2]. At higher temperatures, detailed calculations [3] show aluminized fibres to possess excellent radiation resistance in comparison with unopacified fibres, if the fibre diameter is below 0.1 μm. However, this reference lacks from a correspondence to existing insulation samples. In a theoretical and experimental study of radiation properties of real insulation samples [4], the disagreement between theoretical and measured values of extinction coefficients and thus between calculated and measured radiative conductivity has been attributed to a possible error in applying Beer's law to a transmission measurement without taking into account the scattering in the original beam.

An improved analysis will be presented in this paper. Our theoretical results will be brought into a closer relation to measured IR spectra, as three- and five-flux formulas following from the discrete ordinate method [5, 6], are used. Transmission measurements will be performed with and without the inclusion of scattered radiation. Monte Carlo analyses demonstrate furthermore the validity of the diffusion approximation for strong forward scattering and three- and five-flux formulas as good approximations for solutions of the equation of transfer. For the optimization of a thermal

NOMENCLATURE

a_i	weights for quadrature formula
a_j, b_j	scattering coefficients
A	geometrical cross-section
d	diameter
E	total extinction coefficient
E_Λ	spectral extinction coefficient
E^*	effective extinction coefficient
E_{cal}	calorimetric extinction coefficient
I	intensity
m_Λ	spectral complex index of refraction
n	real part of index of refraction
N	particle density
$p(\theta)$	phase function
$P_i(x)$	Legendre polynomials
$P_n^{(0,1)}(x)$	Jacobi polynomial
$\dot{q}$	total heat flux
$\dot{q}_{sc}$	heat flux due to solid conduction
$\dot{q}_{rad}$	heat flux due to radiation
Q	relative cross-section
r	reflectance
t	transmittance
T	temperature
T_r	mean radiation temperature
x	depth.

Greek symbols

α	dimensionless parameter in Mie theory
δ	angle relative to the normal of the plane
θ	scattering angle
λ	thermal conductivity
Λ	wavelength
μ	$\cos(\theta)$
$\bar{\mu}$	asymmetry factor
μ_i	divisions for quadrature formula
π	porosity
πF	radiation flux
ρ	density of insulation
ρ_0	density of solid fibre
σ	Stefan–Boltzmann constant
σ_s	surface density
τ	optical depth
τ_0	optical thickness
Φ	azimuthal angle, or tilt angle
ω_0	albedo
ω_i	moments of phase function.

insulation it is not sufficient to thoroughly study the magnitude of total heat transfer. Primarily, it is the variety of different heat transfer modes, i.e. solid thermal conductivity, gas conductivity and radiation heat flow, as well as their dependence on residual gas pressure, porosity, fibre or particle diameter, total radiation extinction coefficient and scattering phase function, that have to be investigated separately. Especially a wavelength resolved optical determination of the extinction E and a knowledge of scattering phase functions are indispensable.

2. DETERMINATION OF RADIATIVE CONDUCTIVITY FROM CALORIMETRIC MEASUREMENTS

2.1. *An experimental example*

Figure 1 shows the results of total thermal conductivity measurements of a load-bearing evacuated glass-fibre insulation as a function of temperature. The guarded hot plate device (metering section 0.25 m^2) is described elsewhere [7]. The properties of the tested insulation are: thickness 3 cm, fibre diameter $d = 0.5$–$0.7\,\mu m$, density $\rho = 280\,kg\,m^{-3}$, porosity $\pi = 0.9$. From these results an experimental mean radiation extinction, E_{cal}, of the insulation can be obtained, according to the equation

$$\lambda = \lambda_{sc} + 16n^2\sigma T_r^3/(3E_{cal}) \qquad (2)$$

where $T_r^3 = (T_1^2 + T_2^2)\cdot(T_1 + T_2)/4$, and T_1, T_2 are the temperatures of the hot and cold boundary, respectively. In Fig. 1 the slope of the graph yields $E_{cal} = 14\,900\ m^{-1}$ or the specific extinction $E_{cal}/\rho = 0.053\ m^2\,g^{-1}$ (taking $n^2 = 1.1$). The solid conductivity of the load bearing insulation, which is assumed to be temperature independent, is then determined to $\lambda_{sc} = 1.9 \times 10^{-3}\ W\,m^{-1}\,K^{-1}$. It has the same order of magnitude as the radiative conductivity at $T = 600$ K. The application of equation (2) is valid only, if E is independent of temperature. To check this assumption, it is necessary to know the spectral dependence of extinction, E_Λ. This can either be obtained from an optical experiment *or*, if the index of refraction of the material and its particle geometry is known, by application of Mie scattering theory.

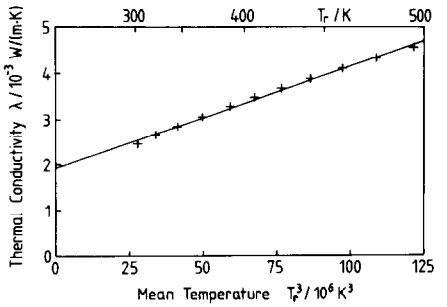

FIG. 1. Calorimetric determination of total thermal conductivity of an evacuated glass-fibre insulation, λ, as a function of effective temperature, T_r. Solid conductivity is assumed to be temperature independent, and the radiative conductivity to be proportional to T_r^3.

2.2. *Validity of radiative diffusion equation*

The diffusion model, which is valid for large optical thicknesses, τ_0, predicts a simple relation between radiative flux $\dot{q}_{rad}$ and extinction coefficient for the case of isotropic scattering [scattering phase function $p(\theta)$ = const.] as given in equations (1) and (2). Note that $\dot{q}_{rad}$ is independent of the albedo, ω_0, the ratio of scattering and extinction coefficients. Compared with isotropic scattering, anisotropic scattering in the forward direction, however, increases the radiation flux significantly. The phase function $p(\theta)$, which indicates the probability of scattering in a specific direction θ off the incoming beam can be expressed as a sum of Legendre polynomials $P_i(\cos\theta)$

$$p(\theta) = \sum_{i=0}^{\infty} \omega_i P_i(\cos\theta) \tag{3}$$

where

$$P_0(\mu) = 1, \quad P_1(\mu) = \mu, \ldots;$$

$$\omega_0 = (1/2)\int_{-1}^{1} p(\mu)\,d\mu,$$

$$\omega_1 = (3/2)\int_{-1}^{1} p(\mu)\mu\,d\mu, \ldots$$

and $\mu = \cos\theta$.

As in neutron diffusion theory [8], the diffusion solution for anisotropic scattering has a similar form as given in equation (1): The extinction E can be replaced by an effective extinction $E^* = E\cdot(1-\bar{\mu})$, where $\bar{\mu} \equiv \overline{\cos\theta} = (1/2)\int_{-1}^{1} p(\mu)\mu\,d\mu$ is the asymmetry factor. With $\bar{\mu} > 0$, $E^* < E$ holds, and thus an increase of λ_{rad} occurs. $\bar{\mu}$ can be indentified as $\omega_1/3$. Thus it is sufficient to know the first moment $\omega_1(\Lambda)$ of the scattering phase function $p(\theta, \Lambda)$ and the extinction coefficient, E_Λ, to determine the radiative heat flux through the insulation.

In order to verify the validity of the diffusion approximation also for *strong* anisotropic scattering, we have performed Monte Carlo simulations [9] (Fig. 2) with a model phase function (Fig. 3, dashed curve) defined as $p(\theta) = \pi/\theta^*$ for $0 \leqslant \theta < \theta^*$ and $p(\theta) = 0$ for $\theta^* \leqslant \theta \leqslant \pi$ where $\theta^* = \pi/6$ is assumed. The procedure is as follows: A photon is emitted from the boundary

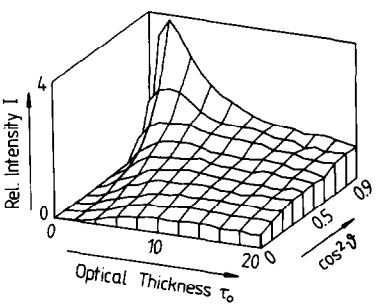

FIG. 2. Relative directed intensity $I(\delta, \tau_0)$ from Monte Carlo simulation for different exit angles with respect to the normal of a plane parallel probe of optical thickness τ_0. Scattering phase function is given in Fig. 3 (dashed line). A parallel incoming beam with normal incidence ($\delta = 0$) is assumed.

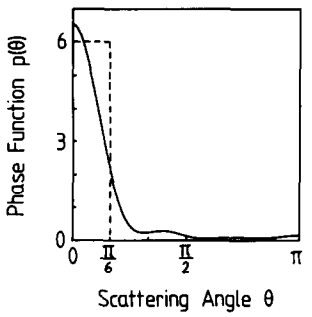

FIG. 3. Model phase function used for the Monte Carlo calculation in Fig. 2 (dashed line), and phase function of a glass fibre with $d = 2$ μm and $\Lambda = 2$ μm (solid line).

$\tau = 0$ with direction $\delta = 0$ and azimuth $\phi = 0$. It is travelling a randomly given optical depth $\Delta\tau = -\cos\delta\cdot\ln(RND)$, where RND is a random number from the random number generator of a TRS-80 microcomputer ($0 < RND \leqslant 1$). The new direction δ' due to the following scattering process is given by $\cos\delta' = \cos\delta\cdot\cos\theta + \sin\delta\cdot\sin\theta\cdot\cos(2\pi\cdot RND)$. The new azimuthal angle ϕ' is not of interest and is set equal to zero. The scattering angle θ is given here [assuming a randomly orientated cylinder with perpendicular incidence and the above model phase function $p(\theta)$] by $\theta = (\pi/6)\cdot RND$. This procedure is repeated until the photon is beyond $\tau = \tau_0$, which means transmission, or $\tau < 0$, which means reflection. As several thousand photons are started during each run, the statistical error due to the finite number of transmission and reflection events is usually below 5%.

In Fig. 2 a parallel radiation beam is assumed to fall onto a sample with normal incidence. With increasing optical thickness, τ_0, the angular distribution of the transmitted intensity is soon smoothed out although $\bar{\mu} = 0.955$! For a similar calculation the phase function of a glass fibre (Fig. 3, solid line) with $d = 2$ μm and for $\Lambda = 2$ μm is used in Fig. 4 ($\bar{\mu} = 0.84$). It shows the emerging intensity distribution after passage through the layer τ_0 for a diffuse radiation field hitting the boundary $\tau = 0$. From both Figs. 2 and 4 the surprising result is a very broad, slightly forward accented intensity distribution though strong asymmetric phase functions or a narrow pencil of incident radiation were

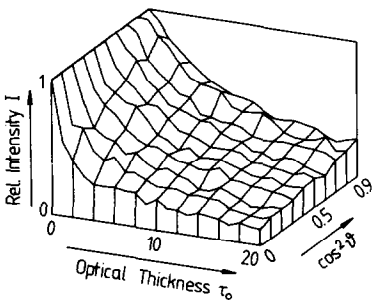

FIG. 4. Relative directed intensity $I(\delta, \tau_0)$ as in Fig. 2 using the phase function of Fig. 3 (solid line). Here, however, a diffuse radiation field is impinging on the probe.

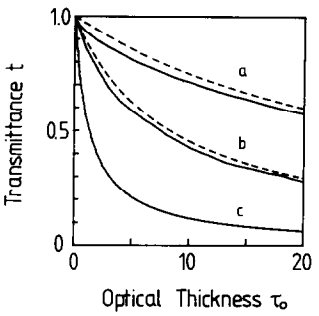

FIG. 5. Total transmitted flux t from Monte Carlo calculations for a diffuse radiation field impinging onto the probe (solid lines); curve (a) using the phase function as in Fig. 3 (dashed line); curve (b) phase function as in Fig. 3 (solid line); curve (c) isotropic phase function $p(\theta) = 1$, for comparison. The dashed lines are the predictions of the linear anisotropic model [equation (4), here $\bar{\mu} = 0.955$, 0.84 and 0, respectively].

used. This demonstrates the diffusion model to be more widely applicable than assumed up to now, i.e. in strong anisotropic scattering cases.

The integrated transmitted flux, t (from Fig. 4), is plotted in Fig. 5 and compared with

$$t = 1/(1+0.75\cdot\tau_0\cdot(1-\bar{\mu})) \tag{4}$$

(linear anisotropic model, compare e.g. ref. [4]) which for large τ_0 is asymptotically equal to the diffusion solution. The agreement is very good especially for large τ_0.

As the diffusion solution has above been demonstrated as a good approximation for radiative heat transfer in a plane parallel, optically thick insulation also for strong anisotropic scattering, only E_Λ and $\bar{\mu} = \omega_1(\Lambda)/3$ are necessary to determine λ_{rad}. For cylindrical and spherical geometries the spectral extinction E_Λ and moment $\omega_1(\Lambda)$ can be calculated numerically from Mie theory (see e.g. Kerker [10]) if the complex index of refraction $m(\Lambda)$ and particle diameter d are known.

2.3. *Mie theory*

Mie theory predicts the relative cross-sections for extinction, Q_{ext}, absorption, Q_{abs}, and scattering, Q_{sc}, of spherical and cylindrical particles, as well as their scattering phase functions $p(\theta)$. From these properties the radiative heat flux in an absorbing, scattering and re-emitting medium can be determined. The extinction coefficient, E_Λ, is connected to the relative extinction cross-section, Q_{ext}, by $E_\Lambda = NAQ_{ext}(\Lambda, d)$, where N is the particle density, A the geometrical cross-section. For cylinders lying perpendicular to the incoming radiation

$$E_\Lambda/\rho = (1/\rho_0)\cdot(4/\Lambda)\cdot Q_{ext}/\alpha \tag{5}$$

where $\alpha = \pi d/\Lambda$, and ρ_0 is the density of the solid cylinder. From E_Λ an averaged mean E_R (applying the Rosseland mean [9]) of the thermal spectrum at temperature T can be evaluated.

Because the tested samples are made of many layers of thin glass-fibre papers, the main radiation flux is perpendicular to the fibre. Therefore, we preliminary use only the case of perpendicular incidence for the numerical calculation. The cross-section for oblique incidence with tilt angle ϕ varies approximately with $\cos\phi$ [11]. Therefore, as a first approximation, the extinction cross-section, Q_{ext}, can be multiplied by $\int_0^{\pi/2}\cos\phi\cdot\cos\phi\,d\phi = \pi/4 = 0.785$ to account for randomly distributed cylinders in the fibre insulation. $\bar{\mu} = \omega_1/3$ can be obtained analytically by integrating the phase function for perpendicular incidence ($\phi = 0$), which yields

$$\bar{\mu} = \left[3(\bar{a}_0 a_1 + \bar{b}_0 b_1) + \sum_{j=1}^{\infty}\bar{a}_j(a_{j-1}+a_{j+1}) + \bar{b}_j(b_{j-1}+b_{j+1})\right] \Big/ (\alpha\cdot Q_{ext}) \tag{6}$$

where a_j, b_j are the scattering coefficients as defined in Kerker [10].

The index of refraction, m_Λ, of glass does not vary appreciably with the chemical composition, as was pointed out by several authors [3, 10]. We used the complex index of refraction of silicate glass from 1 to 30 μm published by Hsieh and Su [12]. Figure 6 shows the calculated specific extinction coefficient, E/ρ, and effective extinction coefficient, E^*/ρ, of glass ($d = 2$ μm, $\rho_0 = 2700$ kg m^{-3}) for perpendicular incidence. It demonstrates that due to strong forward scattering a much smaller effective extinction coefficient E^* (for $\Lambda < 5$ μm) results as could be expected from the huge extinction cross-section E.

Figures 7(a) and (b) show the temperature-dependent specific extinction coefficient vs temperature T and fibre diameter, assuming isotropic scattering (a) and anisotropic scattering (b), respectively. In the first case the maximum is in the range 3–4 μm (depending on temperature). In the latter case, $d = 1.2$ μm, yielding $E^*/\rho = 0.096$ m^2 g^{-1} (or 0.075 m^2 g^{-1} for average tilt angles), is the best choice for the whole temperature range. The extinction decrease from the maximum is below 20%, however, for diameters between 0.6 and 2 μm, so the fibre size distribution is not of great importance within these limits.

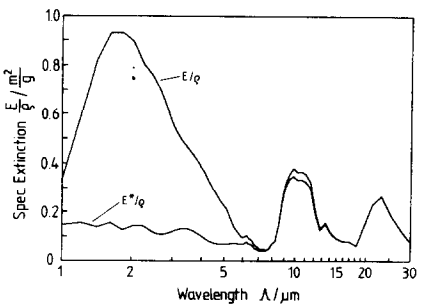

FIG. 6. Specific extinction coefficient, E/ρ, for glass fibres ($d = 2$ μm) predicted by Mie theory for perpendicular incidence, and effective extinction, E^*/ρ, as caused by anisotropic scattering.

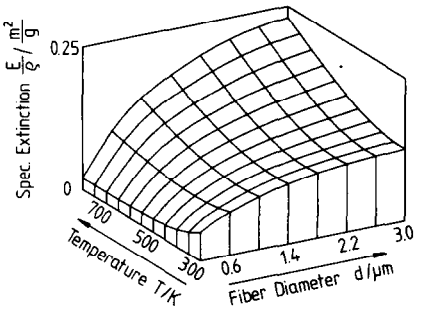

FIG. 7(a). Rosseland mean of specific extinctions, E/ρ, as derived from Mie theory, assuming isotropic scattering, in dependence of temperature T and fibre diameter d.

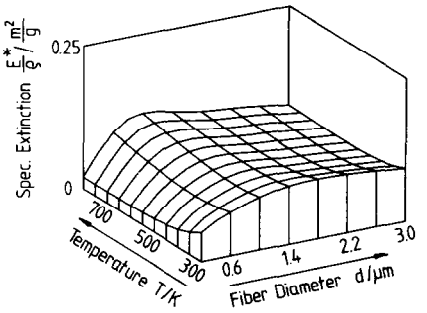

FIG. 7(b). Rosseland mean E^*/ρ as in Fig. 7(a), however, accounting for anisotropic scattering.

While d is large, forward scattering has a drastic effect on the average extinction and hence the radiation flux. As d falls below 1 μm Rayleigh scattering and absorption are dominant and thus E and E^* eventually become equal. The temperature-dependent variation of the extinction between $T = 400$ and 700 K does not exceed $\pm 10\%$ for $d \approx 0.6$ μm, thus the assumption of temperature-independent extinction in equation (2) can be justified. Temperature averaged extinctions in this range for $d = 0.5$ and 0.7 μm are $E^*/\rho = 0.060$ and 0.076 $m^2\ g^{-1}$, respectively, or, if oblique incidence is accounted for, $E^*/\rho = 0.047$ and 0.06 $m^2\ g^{-1}$. This is in very good agreement with the experimental value given in Section 2.1 ($E_{cal}/\rho = 0.053\ m^2\ g^{-1}$).

3. EXTINCTION COEFFICIENTS FROM TRANSMISSION MEASUREMENTS

3.1. *Procedure for determination of transmission and reflection*

The remarkable agreement between measured and calculated extinction coefficients shown above indictates that the radiative flux in an insulator can in principle be deduced from theory, i.e. from the optical constants and the internal geometry of the material. Some limitations, however, are given in practice: we did not account explicitly for oblique incidence, the exact equation of radiation transfer in a medium with randomly oriented cylinders, the effect of dependent scattering (Mie theory assumes independent scattering), and other problems related with exact solutions of radiation transfer combined with solid conductivity. Therefore, it is essential to test the correctness of the simplifications used in additional experiments. One purpose is to measure the extinction coefficient for a (nearly parallel) beam penetrating a sample. The beam is always attenuated by a simple exponential decay $e^{-\tau_0}$ (Beer's law), if scattering in the original beam can be avoided. If the surface density, σ_s, is known, this immediately yields the extinction E per density ρ: $E/\rho = \tau_0/\sigma_s$. The experiment also should reveal the total transmittance and reflectance, t and r, which depend on τ_0, ω_0 and the phase function. Then the experiment can be compared with the predictions of Mie theory and solutions of the equation of transfer.

In the experiment an almost parallel beam is falling on a *cold* sample. The equation of transfer for the intensity I (in general wavelength dependent) in a plane-parallel, non-emitting medium, which has to be applied here, is [6]

$$\mu \cdot \mathrm{d}I(\tau,\mu)/\mathrm{d}\tau = -I(\tau,\mu) + (1/2) \times \int_{-1}^{1} I(\tau,\mu') \sum_{j=0}^{\infty} \omega_j P_j(\mu) \cdot P_j(\mu')\,\mathrm{d}\mu' + (F/4) \cdot \exp(-\tau) \cdot \sum_{j=0}^{\infty} \omega_j P_j(\mu). \quad (7)$$

The last term is due to the incoming parallel beam of flux πF, which can be seen as an internal light source. The boundary conditions then are: $I(\tau = 0,\ \mu) = 0$; $I(\tau = \tau_0,\ -\mu) = 0$, where $\mu > 0$. As in astrophysics, a two-flux approximation is frequently used to solve this equation, where the radiation field is divided into a forward and a backward hemisphere. This method can be generalized, if the directions μ are divided into n discrete directions, μ_i, and corresponding weights, a_i. These are used for evaluation of the integral in equation (7) which is converted into a sum of n terms. Kaganer [5] showed that a three-flux approximation in the $\mu = 0$ direction can be reduced to the formalism of two-flux calculations. He also used divisions μ_i and weights a_i of a quadrature formula on the basis of Jacobi polynomials $P_n^{(0,1)}(x)$ (see Table 1 for divisions and weights with $n = 3$ and 5). In the case of isotropic scattering his results are close to exact numerical solutions of the equation of transfer. The linear anisotropic model equation (4) can be verified easily in the three-flux approximation for albedo $\omega_0 = 1$. We found that extending Kaganer's method to *anisotropic* scattering for arbitrary albedo ω_0 and boundary

Table 1. Divisions, μ_i, and weights, a_i, for quadrature formula

n flux	μ_i	a_i
3	$\pm 2/3$	3/4
	0	1/2
5	$\pm(6+\sqrt{6})/10$	$125/(18\cdot(16+\sqrt{6}))$
	$\pm(6-\sqrt{6})/10$	$125/(18\cdot(16-\sqrt{6}))$
	0	2/9

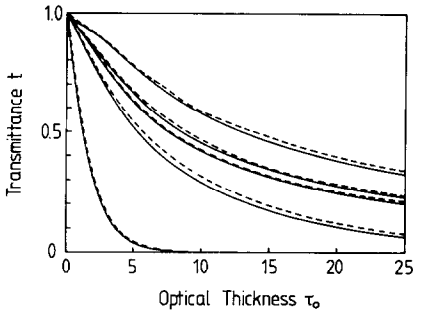

FIG. 8. Comparison of transmittance t derived from Monte Carlo calculations (solid lines) as a function of optical thickness τ_0 and five-flux model (dashed lines). Fibre diameter $d = 2$ μm and wavelengths $\Lambda = 2.5, 3.0, 4.0, 5.0, 6.0$ μm (from top to bottom) are assumed for Mie theory calculations (yielding $\bar{\mu} = 0.86, 0.79, 0.78, 0.72$ and 0.26, respectively).

conditions still yields sufficiently accurate results if five-flux approximations and the first three moments of the phase function $\omega_1 \ldots \omega_3$ are used. Three-flux calculations using ω_1 give satisfying results, if τ_0 is not too small (depending on the asymmetry factor). Five-flux calculations for the case of absorption and anisotropic scattering of a parallel beam falling on a cold medium were performed numerically in order to include also small optical thicknesses into the analysis. Several wavelengths, Λ, and the corresponding phase functions and cross-sections of a 2 μm glass fibre were chosen for demonstration and compared with Monte Carlo calculations (Fig. 8). The good agreement between both theoretical approaches indicate that as Monte Carlo calculations are very time consuming, this five-flux method can be used to compare optical transmissivity measurements with the predictions of Mie theory and radiation transfer theory.

3.2. *Experimental procedure for transmission measurements*

The thermal radiation of a globar (Fig. 9) is focused by a germanium lens on a circular variable filter in the wavelength range 2.5–14.5 μm. A second germanium lens focuses the chopped beam onto the sample. A pyroelectric detector is in close contact with the sample and collects about 75% of the hemispherical IR transmission. The signal is passed to a lock-in amplifier and correlated with the chopper frequency of 12.5 s^{-1}. A semi-reflecting ZnSe-mirror and a second pyroelectric detector enable us to monitor the original intensity.

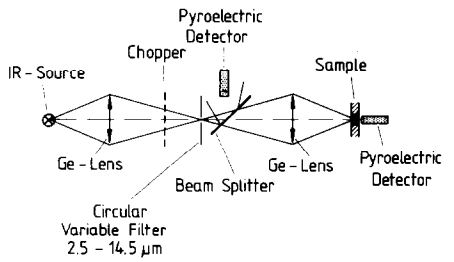

FIG. 9. Experimental setup for IR transmission measurement.

Both signals are digitized and stored in a TRS-80 microcomputer, which is also used to automatically turn the variable filter and a movable detector holder as well as to process and plot the data. In the arrangement described here, the total IR transmission through a sample can be measured.

If the extinction of a fibre-glass sample is to be determined, it is positioned in front of the second lens. Now the scattered radiation is distributed over the hemisphere and only a small fraction arrives at the detector. The dectector, however, still registers the unscattered exponentially attenuated light of intensity I_1. From the primary intensity, I_0, the optical thickness of the sample is derived: $\tau_0 = \ln(I_0/I_1)$. As the detector is 2 mm in diameter and the distance between lens and detector about 60 mm, the scattered intensity hitting the detector is reduced to $(1/60)^2$ or less than 0.03%. Therefore, the influence of scattered light can be neglected. Directed off-beam transmission as well as reflection can be recorded, if the detector is moved around the sample. As no focusing element is used, the maximum distance between detector and sample has to be kept at 2–4 cm.

Various fibre-glass papers have been tested. To get measurable signals in the extinction experiment the papers have to be as thin as possible. The best specimen was Microglass 1000 (Manning Corp., Troy, New York) where sheets of surface densities $\sigma_s = 14.2\ g\,m^{-2}$ could be used. For the transmission experiments usually several sheets were inserted. Prior to measurements, the sheets were heated to 180°C to avoid water absorption in the spectra. Several powders were also studied as candidates for opacifiers. The powders were mixed in small quantities with KBr and pressed into tablets.

4. COMPARISON OF THEORETICAL AND EXPERIMENTAL RESULTS

Figure 10 shows the specific extinction spectrum E/ρ ($\equiv \tau_0/\sigma_s$) of Microglass 1000 and a comparison with Mie calculations for $d = 0.5$, 1.0 and 1.5 μm. A mean size diameter of 0.5 μm is claimed by the manufacturer, SEM-pictures, however, show an appreciable amount

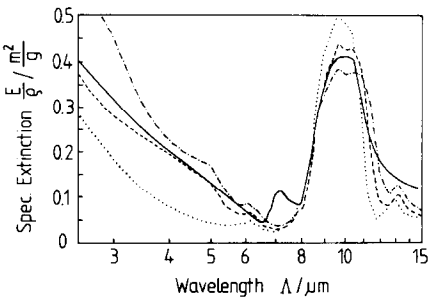

FIG. 10. Comparison between experimental specific extinction, E/ρ, of Microglass 1000 ($\sigma_s = 14.2\ g\,m^{-2}$, solid line), and predictions of Mie theory assuming $d = 0.5$ μm (dotted line), 1.0 μm (dashed line) and 1.5 μm (dashed-dotted line).

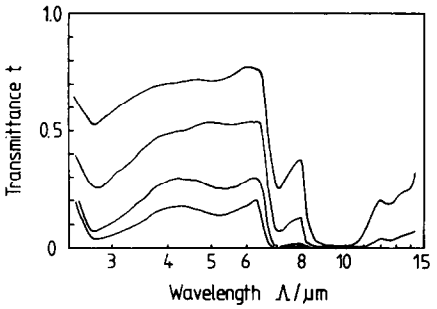

FIG. 11. Measured transmittance, t, vs wavelength for Microglass 1000 with surface densities $\sigma_s = 14.2$, 28.4, 56.8 and 71.0 g m^{-2}, proceeding from top to bottom.

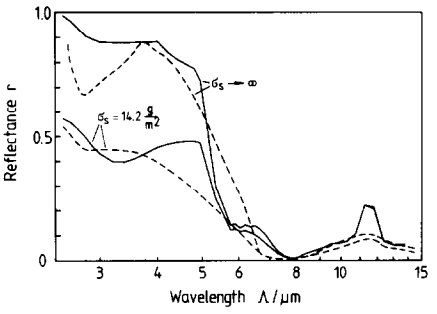

FIG. 13. Measured reflectance (dashed lines) vs wavelength, Λ, for Microglass 1000 with 1 and 12 layers ($\sigma_s = 14.2$ g m^{-2} and $\sigma_s \to \infty$), and predictions from Mie theory and five-flux model (solid lines) assuming $d = 1.4$ μm.

of additional larger fibre sizes in the range of 1 μm. The figure shows a remarkable agreement between measured and calculated spectral extinction. The measured transmittance of several layers of Microglass sheets is shown in Fig. 11. Two different regions have to be distinguished: one of high albedo ω_0 (mainly scattering, $\Lambda \leqslant 6.5$ μm), and the second a strong absorption band around $\Lambda = 10$ μm. Despite a large extinction cross-section at shorter wavelengths (first case), transmittance is large even for *many* layers of Microglass (due to high albedo, ω_0, and forward scattering).

The same wavelengths as in Fig. 8 have been chosen to compare these experimental results with five-flux approximations (Fig. 12). A single fibre diameter of $d = 1.5$ μm is assumed for the Mie calculations of phase functions. The optical thickness was taken from the experimental extinction spectrum (Fig. 10). Experiment and calculation agree and show the reliability of the *ab initio* calculations.

In Fig. 13 the reflectance, r, is plotted for different layers and also compared to the five-flux calculations. In summary, these optically obtained results confirm that forward scattering compared with isotropic scattering indeed enhances radiation flux.

Also, the extinction properties of several powders, which might be suitable as opacifiers were tested experimentally (Fig. 14). As the wavelength region below $\Lambda = 8$ μm is most important for high temperature applications, Fe_3O_4 ($d \approx 0.2$ μm) and $MoTe_2$ ($d \approx 2$ μm) are efficient absorbers. Model calculations for certain weight percents, c, of Fe_3O_4 added to a glass-fibre insulation provided the Rosseland mean of specific extinction coefficients are shown in Fig. 15. The specific extinction of Fe_3O_4 was taken from experimental data (Fig. 14) and combined with the specific extinction, E^*/ρ, obtained from Mie theory calculations (assuming $d = 1$ μm). Especially at higher temperatures T, adding Fe_3O_4 as an opacifier to a fibre-glass insulation increases the total extinction and thus lowers the radiative heat flux appreciably. As the influence of the opacifier Fe_3O_4 to solid conductivity is not known, additional calorimetric heat flux measurements are to be performed.

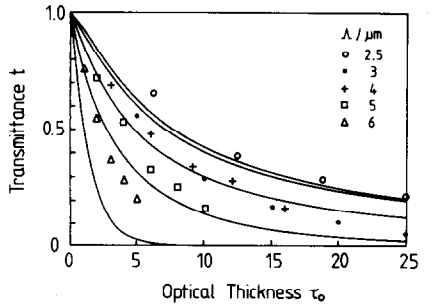

FIG. 12. Comparison of transmittance, t, vs optical thickness, τ_0; wavelengths from transmission experiment as in Fig. 11 (symbols) and theory (solid lines) assuming $d = 1.5$ μm. The optical thickness, τ_0, was taken from experimentally obtained extinction (Fig. 10).

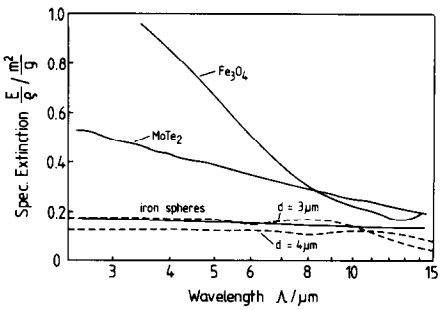

FIG. 14. Experimental specific extinction, E/ρ, vs Λ for Fe_3O_4, $MoTe_2$ and Fe-spheres (solid lines). Prediction of Mie theory for Fe-spheres assuming $d = 3$ and 4 μm (dashed lines).

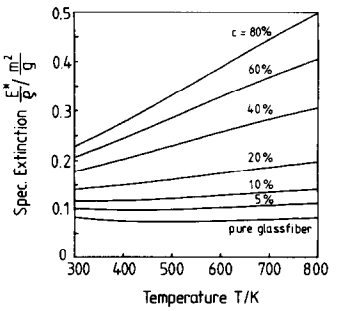

FIG. 15. Specific extinction, E^*/ρ, for glass fibres ($d = 1$ μm) doped with Fe_3O_4 vs temperature T for different concentrations, c, of Fe_3O_4.

Finally a sample of iron spheres (mean diameter as estimated from SEM-pictures $d \approx 4$ μm) was used to compare experimental specific extinction (Fig. 14, lower solid curve) with the prediction from Mie theory for spherical particles (Fig. 14, dashed lines, assuming $d = 3$ and 4 μm). The data of the complex index of refraction for iron are taken from Ordal *et al.* [13], and divided by $n_{KBr} = 1.5$ to take into account the index of refraction of the KBr tablet. Also here a striking agreement between both methods has been found.

REFERENCES

1. H. H. Weber, Über das optische Verhalten von kugeligen, isotropen Teilchen in verschiedenen Medien, *Kolloidzeitschrift* **174,** 66–72 (1960).
2. M. G. Kaganer, *Thermal Insulation in Cryogenic Engineering*, p. 26. Israel Program for Scientific Translations, Jerusalem (1969).
3. K. Y. Wang and C. L. Tien, Radiative heat transfer through opacified fibers and powders, *J. Quant. Spectrosc. Radiat. Transfer* **30,** 213–223 (1983).
4. T. W. Tong and C. L. Tien, Radiative heat transfer in fibrous insulations, *Trans. Am. Soc. Mech. Engrs*, Series C, *J. Heat Transfer* **105,** 70–81 (1983).
5. M. G. Kaganer, Untersuchung der Ausbreitung von Licht im streuenden Medium durch die Methode der diskreten Ordinaten, translated from *Optika Spektrosk.* **26,** 443–449 (1969).
6. S. Chandrasekhar, *Radiative Transfer*, p. 149. Dover, New York (1960).
7. D. Büttner, J. Fricke, R. Krapf and H. Reiss, Measurement of the thermal conductivity of evacuated load-bearing, high temperature powder and glassboard insulations with a 700 × 700 mm² guarded hot plate device, *High Temp.-High Press.* **15,** 233–240 (1983).
8. S. Glasstone and M. C. Edlund, *Kernreaktortheorie*, p. 73. Springer, Wien (1961).
9. R. Siegel and J. R. Howell, *Thermal Radiation Heat Transfer*, p. 608. McGraw-Hill, Tokyo (1972).
10. M. Kerker, *The Scattering of Light*, p. 262. Academic Press, New York (1969).
11. A. C. Lind and J. M. Greenberg, Electromagnetic Scattering by obliquely oriented cylinders, *J. Appl. Phys.* **37,** 3195–3203 (1966).
12. C. K. Hsieh and K. C. Su, Thermal radiative properties of glass from 0.32 to 206 μm, *Solar Energy* **22,** 37–43 (1979).
13. M. A. Ordal, L. L. Long, R. J. Bell, S. E. Bell, R. R. Bell, R. W. Alexander and C. A. Ward, Optical properties of the metals Al, Co, Cü, Au, Fe, Pb, Ni, Pd, Pt, Ag, Ti and Wo in the infrared and far infrared, *Appl. Optics* **22,** 1099–1119 (1983).

PROPRIETES SPECTRALES DE TRANSMISSION ET DE REFLEXION DES MATERIAUX ISOLANTS A HAUTE TEMPERATURE

Résumé—On décrit deux approches pour la détermination du flux radiatif dans les isolants à haute température : (a) étude de la transmission et de la réflexion optique ; (b) application de la théorie rigoureuse de Mie et des simulations Monte-Carlo des mesures calorimétriques et optiques. On montre que le coefficient d'extinction monochromatique *et* le terme du premier ordre du développement en sein de fonction de phase sont indispensables pour une optimisation des propriétés d'isolation d'un isolant anisotropiquement diffusant. Cet article montre la validité de l'approximation de diffusion pour le transfert radiatif aussi pour une diffusion fortement anisotropique. On ajoute une étude des propriétés d'extinction de différents opacifiants.

SPEKTRALE TRANSMISSIONS- UND REFLEXIONSEIGENSCHAFTEN VON HOCHTEMPERATUR-ISOLATIONSMATERIALIEN

Zusammenfassung—Es werden zwei Wege zur Bestimmung des Strahlungsflusses in Hochtemperaturisolationen beschrieben: (a) optische Transmissions- und Reflexionsmessungen; (b) Anwendung der Mie'schen Streutheorie und Monte-Carlo Simulationen von kalorimetrischen und optischen Messungen. Es wird gezeigt, daß die Kenntnis des spektralen Extinktionskoeffizienten und des ersten Terms der Legendrepolynomentwicklung der Streuphasenfunktion ausreichend ist, um die Isolationseigenschaften von anisotrop streuenden Isolationen voraussagen und optimieren zu können. Das Diffusionmodell für den Strahlungstransport behält auch in stark anisotrop streuenden Medien Gültigkeit. Weiterhin werden Extinktionseigenschaften von verschiedenen Infrarot-Trübungsmitteln beschrieben.

СПЕКТРАЛЬНЫЕ ХАРАКТЕРИСТИКИ ОТРАЖЕНИЯ И ПРОПУСКАНИЯ ВЫСОКОТЕМПЕРАТУРНЫХ ИЗОЛЯЦИОННЫХ МАТЕРИАЛОВ

Аннотация—Описаны два метода определения потока излучения высокотемпературных изоляционных материалов: (а) оптический способ определения пропускания и отражения; и (б) использование строгой теории рассеяния Ми и моделирование методом Монте-Карло калориметрических и оптических измерений. Показано, что разрешенный по длине волны коэффициент затухания и член первого порядка в разложении в ряд фазовой функции рассеяния являются необходимыми параметрами для оптимизации изоляционных свойств анизотропно рассеивающего материала. Показана справедливость диффузионной аппроксимации лучистого переноса также в случае сильного анизотропного рассеяния. Кроме того, исследованы параметры затухания в различных непрозрачных материалах.